Measurement of Environmental Radiation with γ Spectroscopy Techniques

Group 25

Rocco Ardino	Francesco Gentile	Matteo De Tullio
Matr. 1231629	Matr. 1239149	Matr. 1225015

14-18-19 November 2019

1 Objectives

- Studying the γ transitions in some radioactive samples.
- Measuring the activity of the radioactive sources contained in the various samples.

2 Experimental apparatus

The experimental apparatus consisted of:

- A shielded well.
- A NaI(Tl) scintillation detector coupled to a photo-multiplier tube.
- A high purity Ge scintillation detector.
- A digitizer with two channels, for the two detectors, with a trapezoidal filter which reshapes the incoming signal.
- Some samples of both organic and inorganic materials, such as pellets and mushrooms.
- A sample of air humidity collected with a canister.
- Some samples of known radionuclides such as ^{22}Na, ^{241}Am, ^{152}Eu.

3 Trapezoid Filter Setting

In order to estimate the energy, we cannot integrate on the incoming signal because it is too large. We need to reshape it with a trapezoidal filter. First, we set the *threshold* on the signal amplitude, i.e. the amplitude value above which the signal is acquired. Then we chose the parameters to be given as input to the trapezoidal filter in order to optimize the resolution of both detectors. Such parameters were:

- **Decay Time**, which is an estimate of the average decay time of the observed signals to be given as input to the filter.
- **Trapezoid Rise Time**, which is the desired time for the rise of the trapezoid shape.
- **Trapezoid Flat Top**, which is the desired time for the flat part on the top of the trapezoid shape.

Eventually a rescaling parameter can be chosen in order to better observe the trapezoid shape on the screen. The parameters we chose are shown in Table 1.

Parameter	NaI(Tl) channel	HPGe channel
Threshold [mV]	20	500
Decay Time [μs]	120	4
Trapezoid Rise Time [μs]	0.5	0.3
Trapezoid Flat Top [μs]	0.3	0.1

Table 1: Trapezoid Filter Parameters.

4 Detector Calibration

Data Acquisition We acquired for 10 minutes the spectra of the radioactive sources ^{22}Na, ^{241}Am, using the NaI detector, and for 20 minutes the one from ^{152}Eu using the HPGe detector. The reason for this choice was that ^{152}Eu has many peaks which can be clearly distinguished

only with the HPGe detector because it has a higher resolution than the NaI(Tl) one. The sources were placed in front of each detector at the following distances:

$$\Delta L_{\mathrm{NaI(Tl)}} = 21 \text{ cm} \qquad \Delta L_{\mathrm{HPGe}} = 29 \text{ cm} \tag{1}$$

Data Analysis Given the acquired spectra, we identified the peaks corresponding to the γ emissions and fitted them with a gaussian in order to get the value of their centroid μ and standard deviation σ. Then we computed the energy resolutions of each peak as follows:

$$R = \frac{\mathrm{FWHM}_\mu}{\mu} = \frac{2.355 \cdot \sigma}{\mu}. \tag{2}$$

Since the energy axis was given in arbitrary units, as output from the electronics, we associated to the peak means the expected values in keV[1]. The energies of the peaks, their centroids μ, standard deviations σ and resolutions R are reported in Table 2.

Source	Detector	E_{expected} [keV]	μ [a.u.]	σ [a.u.]	R [a.u.]
^{22}Na	NaI(Tl)	511	1517 ± 1	73 ± 1	0.114 ± 0.002
^{22}Na	NaI(Tl)	1275	3669 ± 4	135 ± 6	0.086 ± 0.004
^{241}Am	NaI(Tl)	59	203.16 ± 0.05	15.22 ± 0.04	0.1764 ± 0.0005
^{152}Eu	HPGe	121.8	411.34 ± 0.02	3.02 ± 0.02	0.0173 ± 0.0001
^{152}Eu	HPGe	244.7	823.98 ± 0.06	3.65 ± 0.08	0.0104 ± 0.0002
^{152}Eu	HPGe	344.3	1158.68 ± 0.03	3.19 ± 0.02	0.00649 ± 0.00004
^{152}Eu	HPGe	367.8	1236.9 ± 0.2	3.3 ± 0.1	0.0062 ± 0.0002
^{152}Eu	HPGe	411.1	1383.3 ± 0.1	3.1 ± 0.1	0.0053 ± 0.0002
^{152}Eu	HPGe	444.0	1493.6 ± 0.1	3.3 ± 0.1	0.0052 ± 0.0002
^{152}Eu	HPGe	778.9	2618.89 ± 0.08	3.42 ± 0.05	0.00308 ± 0.00004
^{152}Eu	HPGe	867.4	2915.9 ± 0.1	3.5 ± 0.1	0.0028 ± 0.0001
^{152}Eu	HPGe	964.0	3240.8 ± 0.1	3.80 ± 0.08	0.00276 ± 0.00006
^{152}Eu	HPGe	1085.8	3649.8 ± 0.1	4.9 ± 0.1	0.00314 ± 0.00009
^{152}Eu	HPGe	1112.1	3738.2 ± 0.1	3.75 ± 0.08	0.00236 ± 0.00005
^{152}Eu	HPGe	1408.0	4732.46 ± 0.09	4.13 ± 0.06	0.00205 ± 0.00003

Table 2: Energy, Centroid, Sigma and Resolution of the Peaks in the ^{22}Na, ^{241}Am and ^{152}Eu Spectra

We wished to convert the arbitrary units of the energy axis into keV. To do this, we considered the peaks found in the spectra of ^{22}Na and ^{241}Am for the NaI(Tl) detector and those found also in ^{152}Eu for the HPGe detector. Then we fitted the centroid values against the energy expected values in keV, to find the so called calibration coefficients a and b:

$$E_{\mathrm{keV}} = a + b \cdot E_{\mathrm{a.u.}}. \tag{3}$$

The linear fit is shown in Figure 1, whereas the calibration coefficients can be read in Table 3.

[1]The energy values of the peaks were taken from `www.nucleide.org`.

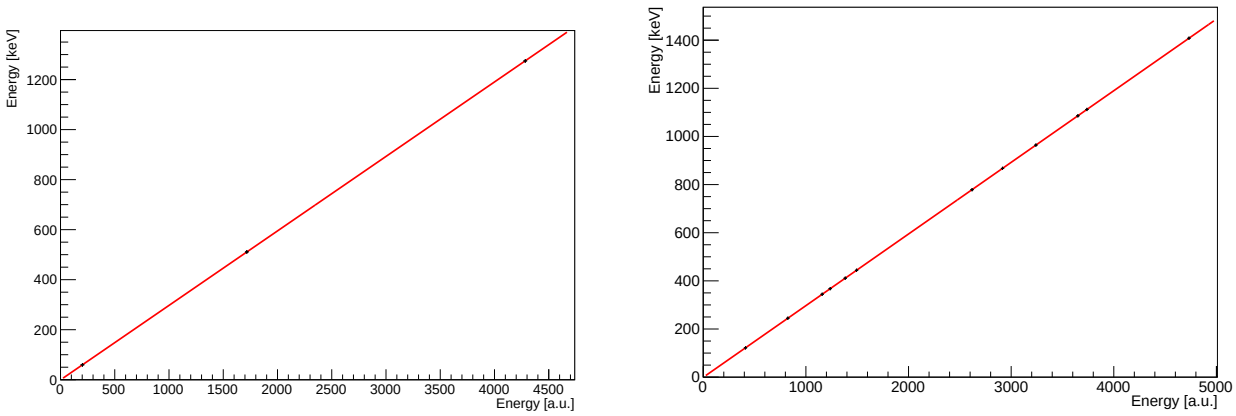

(a) *NaI(Tl) Detector* **(b)** *HPGe Detector*

Figure 1: Calibrations of the detectors. Left: calibration of NaI(Tl) with ^{22}Na and ^{241}Am sources. Right: calibration of HPGe with ^{152}Eu source.

Detector	a [keV]	b [keV/a.u]
NaI	-0.611 ± 0.005	0.29778 ± 0.00002
HPGe	-0.620 ± 0.007	0.29766 ± 0.00001

Table 3: Calibration Coefficients

5 Measurement of Detector Efficiencies

We are now interested at studying the following efficiency parameters:

- The detector intrinsic efficiency ε_{tot}, defined as the ratio between the number of detected events and the number of γ that reached the detector.
- The peak efficiency $\varepsilon_{\text{peak}}$, defined as the ratio between the number of events forming the peak and the number of γ that reached the detector with the energy which characterizes the peak.

Estimate of the number of γ hitting the detector We had the data relative to the current activity of the radioactive sources. In order to get the number of photons hitting the detector at a certain energy, we multiplied the activity A for the acquisition time T, for a geometric factor ϵ_{geom} and for the number of photons per disintegration produced at that fixed energy[2] w:

$$N_\gamma^{\text{tot}} = A \cdot T \cdot \epsilon_{\text{geom}} \cdot w. \tag{4}$$

The geometric factor ϵ_{geom} is defined as the ratio between the solid angle seen by the detector and the one corresponding to the sphere:

$$\epsilon_{\text{geom}} = \frac{1}{4\pi} \cdot \frac{\pi R^2}{\Delta L^2}, \tag{5}$$

where R is the radius of the detector and ΔL is the distance between source and detector figuring in Equation 1. Table 4 shows the geometric parameters of the detectors useful for the

[2]The weights are taken from `http://www.nucleide.org/DDEP_WG/DDEPdata.htm`

calculation of ϵ_{geom}, whereas Table 5 shows the activity and the acquisition time associated to each of the sources. In Table 6 the final estimates of the total number of γ hitting the two detectors for each source are exposed.

Detector	Radius [mm]	Distance from Source [mm]	Geometric Factor
NaI(Tl)	37.5	210	$8.19 \cdot 10^{-3}$
HPGe	38	290	$4.30 \cdot 10^{-3}$

Table 4: Detector Geometric Parameters

Source	Activity [kBq]	Acquisition Time [min]
^{22}Na	0.95	10
^{241}Am	374.0	10
^{152}Eu	91.0	20

Table 5: Activity and Acquistion Time per Source

Source	Energy (keV)	Weight w	Number of γ hitting NaI(Tl)	Number of γ hitting HPGe
^{22}Na	511	1.810	$8.4 \cdot 10^3$	$4.4 \cdot 10^3$
^{22}Na	1275	1.000	$4.7 \cdot 10^3$	$2.4 \cdot 10^3$
^{241}Am	59	0.36	$6.6 \cdot 10^5$	$3.5 \cdot 10^5$
^{152}Eu	121.8	0.2841	$2.5 \cdot 10^5$	$1.3 \cdot 10^5$
^{152}Eu	244.7	0.0755	$6.7 \cdot 10^4$	$3.5 \cdot 10^4$
^{152}Eu	344.3	0.2659	$2.4 \cdot 10^5$	$1.3 \cdot 10^5$
^{152}Eu	367.8	0.0086	$7.7 \cdot 10^3$	$4.0 \cdot 10^3$
^{152}Eu	411.1	0.0224	$2.0 \cdot 10^4$	$1.0 \cdot 10^5$
^{152}Eu	444.0	0.0312	$2.8 \cdot 10^4$	$1.5 \cdot 10^4$
^{152}Eu	778.9	0.1297	$1.2 \cdot 10^5$	$6.1 \cdot 10^4$
^{152}Eu	867.4	0.0424	$3.8 \cdot 10^4$	$2.0 \cdot 10^4$
^{152}Eu	964.0	0.1463	$1.3 \cdot 10^5$	$6.9 \cdot 10^4$
^{152}Eu	1085.8	0.1015	$9.1 \cdot 10^4$	$4.8 \cdot 10^4$
^{152}Eu	1112.1	0.136	$1.2 \cdot 10^5$	$6.4 \cdot 10^4$
^{152}Eu	1408.0	0.2085	$1.9 \cdot 10^5$	$9.8 \cdot 10^4$

Table 6: Estimate of the Total Number of Photons hitting the Detectors.

Estimate of Intrinsic Efficiencies We first needed to subtract the background to the spectra acquired in Section 4. We took a background acquisition lasting 50 minutes and we normalized such spectrum to the time of each acquisition of the spectra of the radioactive sources. After that, we first integrated over each peak's range, in order to get the number of events forming the peak. Then we summed all the counts associated to each peak in order to obtain the total number of events revealed by the detector. At this point we were ready to calculate, both the total efficiencies and the peak efficiencies, as:

$$\epsilon_{\text{tot}} = \frac{\sum_{\text{peaks}} N_{\text{peak}}}{\sum_{\text{energies}} N^{\gamma}_{\text{energy}}} \qquad \epsilon_{\text{peak}} = \frac{N_{\text{peak}}}{N^{\gamma}_{\text{energy}}} \tag{6}$$

The values of the peak efficiencies are exposed in Table 8, whereas Figure 2 shows the behaviour of the intrinsic efficiencies as a function of the energy for the sources ^{22}Na and ^{241}Am. The efficiency plot for the ^{152}Eu will be discussed in the following paragraph.

Source	Total Efficiency in HPGe	Total Efficiency in NaI(Tl)
^{22}Na	0.023 ± 0.001	0.53 ± 0.01
^{241}Am	0.613 ± 0.001	0.211 ± 0.001
^{152}Eu	0.267 ± 0.001	**

Table 7: Total Efficiencies.

Source	Energy(keV)	Peak Efficiency in HPGe	Peak Efficiency in NaI(Tl)
^{22}Na	511	0.0435 ± 0.0003	0.125 ± 0.001
^{22}Na	1275	0.0303 ± 0.0003	0.062 ± 0.001
^{241}Am	59	0.0751 ± 0.0002	0.3142 ± 0.0005
^{152}Eu	121	7.28 ± 0.08	**
^{152}Eu	244	4.67 ± 0.06	**
^{152}Eu	344	3.37 ± 0.04	**
^{152}Eu	367	3.1 ± 0.1	**
^{152}Eu	411	2.51 ± 0.06	**
^{152}Eu	444	2.52 ± 0.05	**
^{152}Eu	778	1.57 ± 0.02	**
^{152}Eu	867	1.27 ± 0.03	**
^{152}Eu	964	1.33 ± 0.02	**
^{152}Eu	1085	1.29 ± 0.02	**
^{152}Eu	1112	1.24 ± 0.02	**
^{152}Eu	1408	1.00 ± 0.02	**

Table 8: Peak Efficiencies. The ones for ^{152}Eu source are normalized to the efficiency for 1408 keV γ.

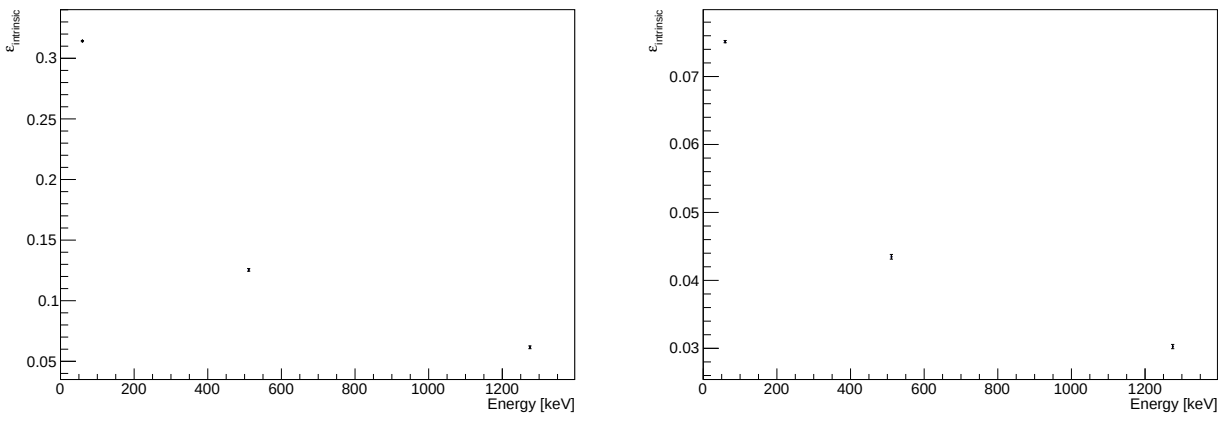

(a) *NaI(Tl) Detector* **(b)** *HPGe Detector*

Figure 2: Peak efficiencies *vs* Energies.

Reconstruction of the relative efficiency curve of the Germanium detector In order to reconstruct the relative efficiency curve of the Germanium detector, we considered the ^{152}Eu

spectrum and assumed that the 1408 keV peak had an efficiency of 100%. Then, all the other efficiencies were referred to this value.

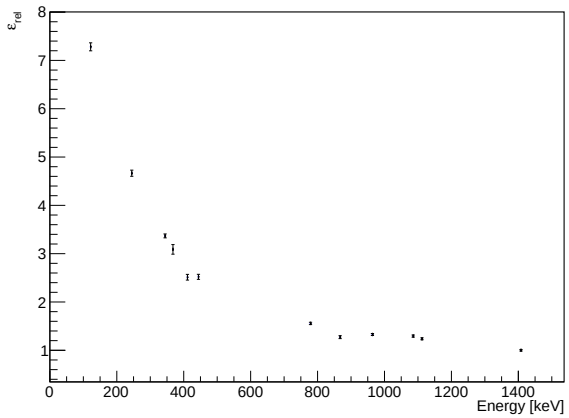

Figure 3: Relative efficiency curve for HPGe detector and ^{152}Eu source.

6 Gamma decay for some samples

We analyzed some samples, listed in Table 9, with the aim of identifying the elements emitting γ rays and of measuring the activity of each source.

Sample	KCl	H_2O	Pellet	Mushrooms (^{137}Cs source)	Autunite
Weight [g]	8	500	193.9	16.6	29

Table 9: Radioactive samples with their masses.

Data Acquisition We acquired the γ spectra of each sample for 15 minutes, except for the Autunite samples, for which the acquisition lasted 30 minutes. Then we proceeded to the acquisition of the background for 15 minutes. After that, the various spectra were calibrated using the results obtained in Section 4 after checking that the calibration coefficients had not changed. Finally we subtracted the background to each of the spectra, taking into account the fact that the acquisitions were taken in different times. To do so, we multiplied the background spectrum for the ratio between the sample and the background acquisition time. In the following Figures, the results are reported for every sample.

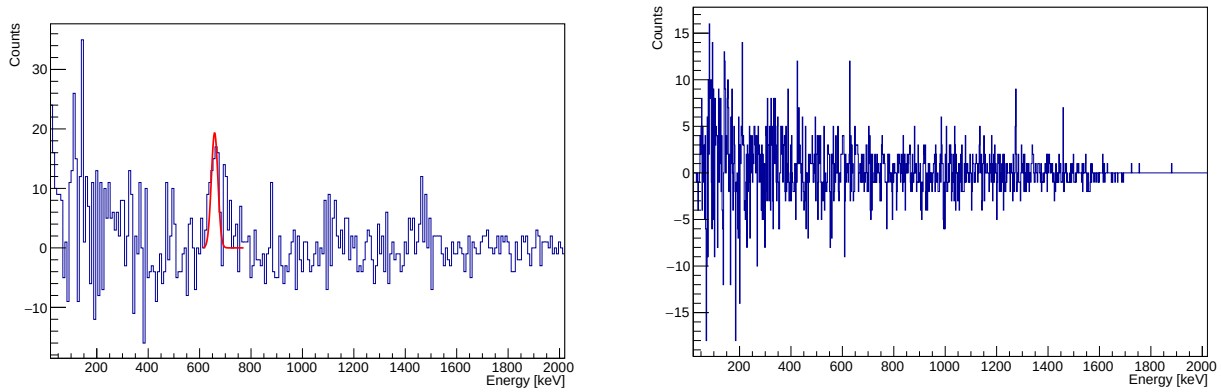

(a) *NaI(Tl) Detector* **(b)** *HPGe Detector*

Figure 4: Mushrooms sample spectra from both detector.

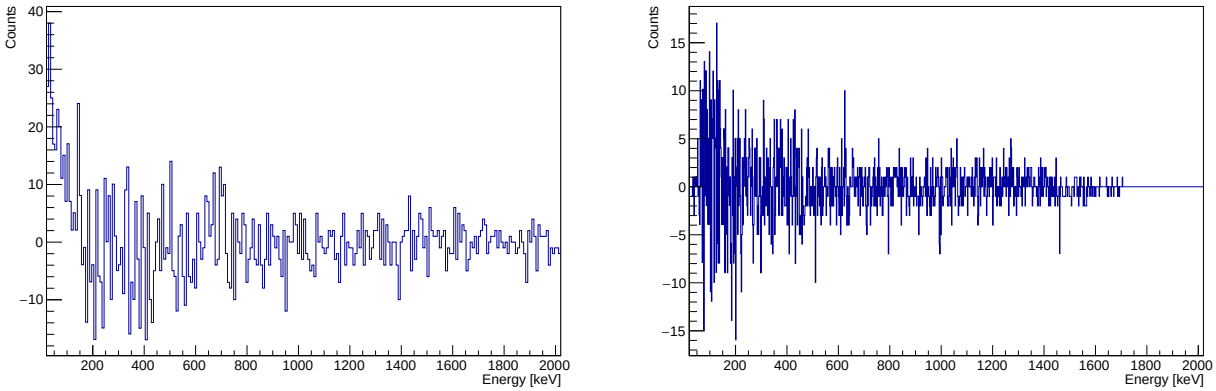

(a) *NaI(Tl) Detector* **(b)** *HPGe Detector*

Figure 5: Pellets sample spectra from both detector.

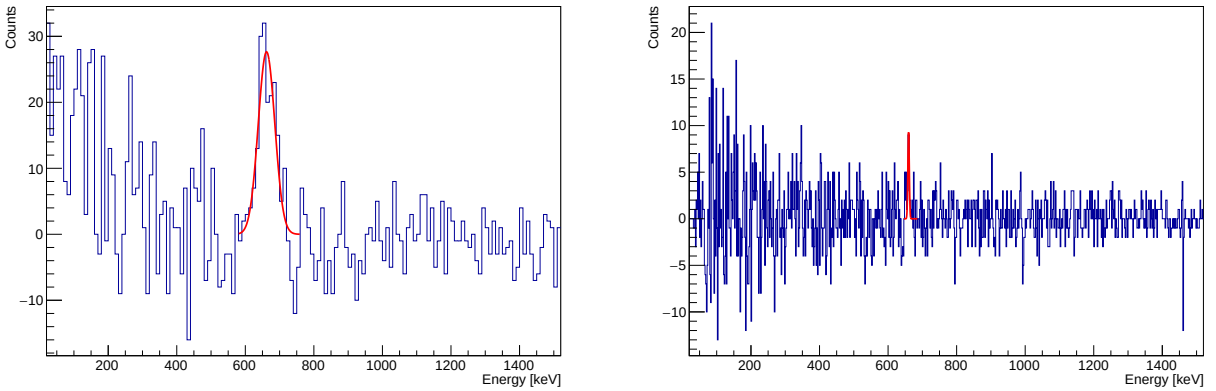

(a) *NaI(Tl) Detector* **(b)** *HPGe Detector*

Figure 6: H_2O sample spectra from both detector.

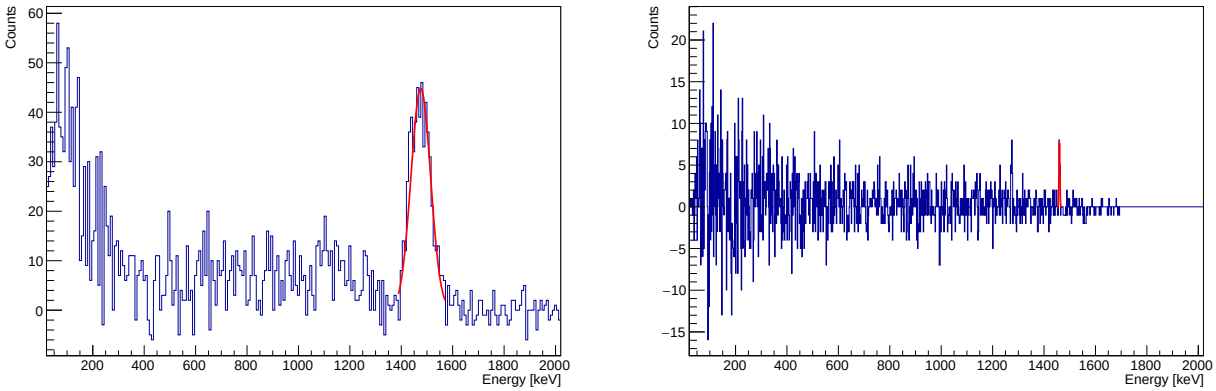

(a) *NaI(Tl) Detector* **(b)** *HPGe Detector*

Figure 7: KCl sample spectra from both detector.

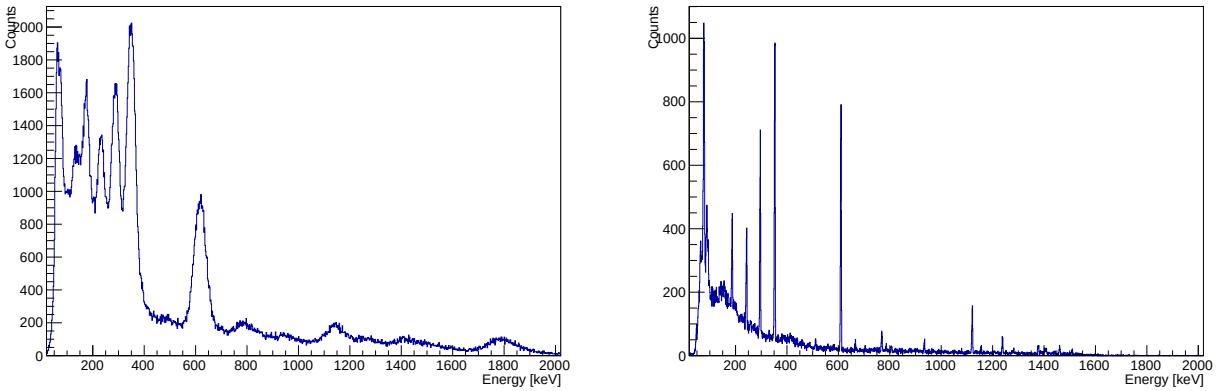

(a) *NaI(Tl) Detector* **(b)** *HPGe Detector*

Figure 8: Autunite sample spectra from both detector.

Identification of the γ emitted by each source and measurement of the Activity Once the calibrations and the background subtraction operations had been carried out, we looked at each spectrum and identified the peaks corresponding to γ emissions. Through a gaussian fit, we measured the centroid μ and the sigma σ associated to each peak. Then, we tried to assign to each peak the known energy of γ rays, characterising one of the radioactive elements naturally present on Earth. Finally, we tried to estimate the activities per unit mass of the samples, which are given by the following expression:

$$\text{Act}_{\text{source}} = \frac{\text{Counts}}{\Delta t \cdot m \cdot \epsilon \cdot R \cdot \epsilon_{\text{geom}}}. \tag{7}$$

where:

- Δt is the acquisition time,
- m is the mass of the sample,
- ϵ is the intrinsic efficiency of the detector measured in Section 5,
- R is the branching ratio associated to the decay,[3]
- ϵ_{geom} is the geometrical factor defined in section 5 and recalculated with the new distances of the samples from the detectors:

$$L_{\text{NaI(Tl)}} = 2{,}5 \text{ cm} \Longrightarrow \epsilon_{\text{geom}} = 0{,}375$$
$$L_{\text{HPGe}} = 9 \text{ cm} \Longrightarrow \epsilon_{\text{geom}} = 0{,}104$$

The results are reported in Table 10, namely the energy measured for each peak, the theoretical value, the radionuclide we associated to it and the activity of the source associated to that γ emission. Notice that no peak was found in the pellet spectrum because it was too noisy.

[3]The branching ratios of the γ-decays were taken from `www.nucleide.org`.

Sample	Expected Energy [keV]	Measured Energy [keV]	Branching Ratio	Number of Events [keV]	Activity [Bq/kg]
H_2O (NaI(Tl))	661.7	662 ± 2.0	0.85	180 ± 10	1.0 ± 0.8
H_2O (HPGe)	661.7	659.8 ± 0.4	0.85	40 ± 6	24 ± 3
KCl (NaI(Tl))	1460.8	1475.0 ± 2	0.106	540 ± 20	38000 ± 1000
KCl (HPGe)	1460.8	$1460.1 \pm 0{,}5$	0.106	17 ± 4	8000 ± 300
Mushr. (NaI(Tl))	661.7	658 ± 2	0.85	130 ± 10	6400 ± 500
Autun. (NaI(Tl))	185.7	173.9 ± 0.3	0.57	24700 ± 100	9800 ± 60
Autun. (NaI(Tl))	242	232.5 ± 0.3	0.0725	27100 ± 100	95700 ± 500
Autun. (NaI(Tl))	295.2	287.5 ± 0.2	0.1841	36000 ± 100	55500 ± 200
Autun. (NaI(Tl))	351.9	348.2 ± 0.1	0.356	42400 ± 200	37400 ± 100
Autun. (NaI(Tl))	609.3	617.5 ± 0.2	0.4549	33400 ± 100	33600 ± 100
Autun. (NaI(Tl))	1120.3	1148 ± 1	0.149	13700 ± 100	72500 ± 600
Autun. (NaI(Tl))	1764.5	1790 ± 1	0.058	9300 ± 90	210000 ± 2000
Autun. (HPGe)	185.7	186.62 ± 0.07	0.57	1300 ± 30	6900 ± 100
Autun. (HPGe)	242	242.71 ± 0.06	0.0727	1100 ± 30	50800 ± 1000
Autun. (HPGe)	295.2	296.02 ± 0.04	0.1841	2300 ± 40	43300 ± 800
Autun. (HPGe)	351.9	352.62 ± 0.03	0.356	3600 ± 60	36700 ± 600
Autun. (HPGe)	609.3	609.82 ± 0.03	0.4549	2800 ± 50	27600 ± 500
Autun. (HPGe)	768.4	768.6 ± 0.1	0.049	200 ± 10	22000 ± 1000
Autun. (HPGe)	934.1	934.4 ± 0.2	0.031	100 ± 10	27000 ± 2000
Autun. (HPGe)	1120.3	1120.23 ± 0.09	0.149	600 ± 20	24000 ± 900
Autun. (HPGe)	1238.1	1238.2 ± 0.1	0.058	200 ± 10	23000 ± 1000

Table 10: Measured Energies *vs* Expected Energies and Activities of the sources.

7 Radon Counting

Finally we wanted to identify the γ emissions and measure the associated activity per liter for a sample of air humidity.

Data Acquisition In order to collect a sample of air humidity, we took a canister capable of absorbing water vapor and left it in a storage room for 5 days. We measured the weight of the air humidity by subtracting the weight of the empty canister to that of the canister with vapor. In Table 11 the main characteristics of the air humidity sample are collected.

Time of exposure (h)	**Water gain (kg)**	**Average humidity**
119.8	0.0147	80%

Table 11: Air Humidity Sample features.

First we acquired the spectrum of the air humidity for 30 minutes, then the associated background, using an empty canister. We also had a *calibration sample* of ^{222}Rn to be used as a reference for the calculation of the activity of the air humidity sample.The spectrum of the *calibration sample* was acquired for 30 minutes. Once we had collected all the spectra, we proceeded to their calibration and the background subtraction as it was done in Section 6. Spectra are shown in Figure 9 and 10.

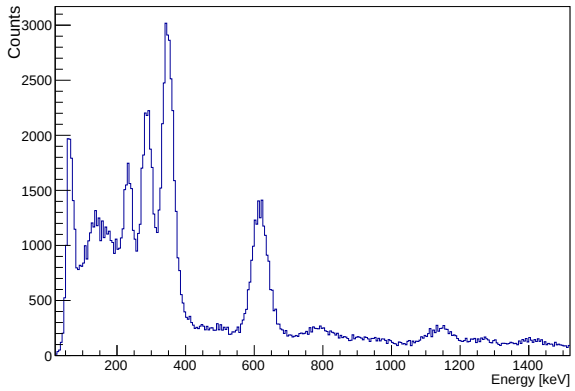

(a) *NaI(Tl) Detector*

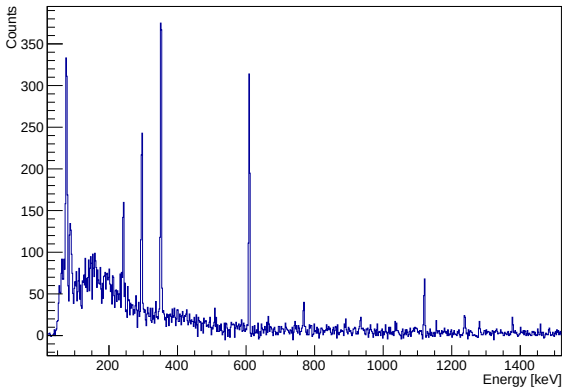

(b) *HPGe Detector*

Figure 9: *Air Humidity Sample* Spectra from both detectors.

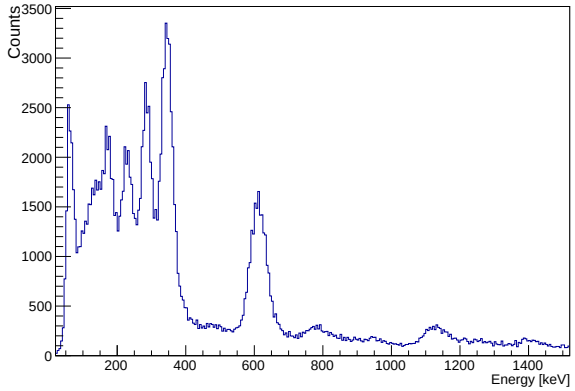

(a) *NaI(Tl) Detector*

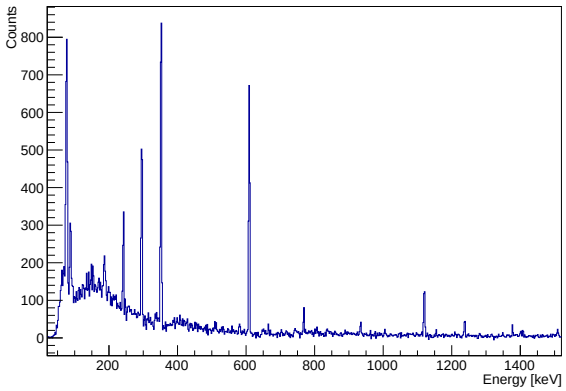

(b) *HPGe Detector*

Figure 10: *Calibration sample* spectra from both detector.

Identification of γ rays We proceeded to the identification of the γ rays emitted by the air humidity sample and the calibration sample. First we measured the peak energies through a gaussian fit, as it was done in Section 6. Then we compared those values with those expected from the ^{222}Rn decay chain. The measured values for the γ emissions are compared to those expected in both the cases of the air humidity sample (Table 12 and 14) and of the calibration sample (Table 13 and 15).

Expected Energy [keV]	Branching Ratio	Measured Energy [keV]	Standard Deviation [keV]	Counts	Compatibility
46.5	4.2 %	65.4 ± 0.1	11.4 ± 0.1	10900 ± 100	1.7
242	7.3 %	232.3 ± 0.2	23.0 ± 0.5	14200 ± 100	0.4
295	18.4 %	287.6 ± 0.2	21.7 ± 0.3	19400 ± 100	0.3
352	35.6 %	347.3 ± 0.2	19.8 ± 0.2	25000 ± 200	0.2
609	45.5 %	616.5 ± 0.3	28.1 ± 0.3	17100 ± 100	0.3
768	4.9 %	785.3 ± 2.1	88.5 ± 4.5	6900 ± 80	0.2
1120	14.9 %	1142.6 ± 2.0	57.5 ± 3.3	4600 ± 70	0.4

Table 12: Measured Energies *vs* Expected Energies for **Air Humidity Sample** - NaI(Tl) Detector.

Expected Energy (keV)	Branching Ratio	Measured Energy (keV)	Standard Deviation (keV)	Counts	Compatibiity
46.5	4.2 %	65.0 ± 0.1	11.8 ± 0.1	13700 ± 100	1.6
242	7.3 %	229.2 ± 0.4	25.5 ± 0.7	17100 ± 100	0.5
295	18.4 %	284.6 ± 0.2	21.6 ± 0.2	21600 ± 200	0.5
352	35.6 %	$344{,}4 \pm 0.2$	19.8 ± 0.2	27900 ± 200	0.4
609	45.5 %	612.1 ± 0.2	28.2 ± 0.3	20000 ± 100	0.1
768	4.9 %	781 ± 2	73 ± 3	6900 ± 80	0.2
1120	14.9 %	1132 ± 5	51 ± 1	5500 ± 70	0.2

Table 13: Measured Energies *vs* Expected Energies for **Calibration Sample** - NaI(Tl) Detector.

Expected Energy [keV]	Branching Ratio	Measured Energy [keV]	Standard Deviation [keV]	Counts	Compatibility
46.5	4.2 %	77.1 ± 0.5	15.6 ± 0.6	2460 ± 50	1.96
242	7.3 %	241.6 ± 0.2	4.7 ± 0.3	660 ± 30	0.08
295	18.4 %	295.46 ± 0.09	1.99 ± 0.07	640 ± 30	0.23
352	35.6 %	351.78 ± 0.06	1.68 ± 0.05	940 ± 30	0.13
609	45.5 %	609.15 ± 0.07	1.40 ± 0.04	640 ± 30	0.11
768	4.9 %	767.9 ± 0.4	3.8 ± 0.4	140 ± 10	0.03
1120	14.9 %	1120.2 ± 0.2	1.5 ± 0.1	140 ± 10	0.11

Table 14: Measured Energies *vs* Expected Energies for **Air Humidity Sample** - HPGe Detector.

Expected Energy (keV)	Branching Ratio	Measured Energy (keV)	Standard Deviation (keV)	Counts	Compatibility
46.5	4.2 %	77.7 ± 0.3	14.8 ± 0.3	5550 ± 70	2.11
242	7.3 %	241.4 ± 0.3	6.2 ± 0.4	1250 ± 40	0.09
295	18.4 %	295.33 ± 0.05	2.01 ± 0.06	1460 ± 40	0.16
352	35.6 %	351.85 ± 0.04	1.79 ± 0.04	2050 ± 50	0.08
609	45.5 %	609.08 ± 0.04	1.53 ± 0.03	1460 ± 40	0.05
768	4.9 %	769.6 ± 0.6	4.6 ± 0.4	280 ± 20	0.35
1120	14.9 %	1119.9 ± 0.1	1.83 ± 0.08	320 ± 20	0.07

Table 15: Measured Energies *vs* Expected Energies for **Calibration Sample** - HPGe Detector.

We can see that there is very good agreement between the energies measured for the calibration sample and for the air humidity one. The agreement is acceptable between measured and expected value: we might improve such result by improving the calibration in order to have more reliable experimental values.

Activity Measurement The procedure for estimating the activity per liter, instead, was different. Following the EPA standards, we computed the activity per liter as follows:

$$\frac{\text{Act}_{\text{Rn}}}{\text{liter}} = \frac{N}{E \cdot CF \cdot DF \cdot T_{\text{exposure}}}, \tag{8}$$

where:

- N is the number of counts per week per pCi obtained summing all the γ events in the spectra of the exposed canister;
- E is the total number of counts per week per pCi, obtained summing up all the γ transitions for the standard calibration source;
- T_{exposure} is the exposure time for the canister (it has to be expressed in minutes);
- CF is a calibration factor which indicates how many liters of air are presumably filtered per minute from the canister during the exposure. It was estimated in this way:

$$CF = \frac{CF_{\text{standard}}}{AF_{\text{standard}}} \cdot AF(T_{\text{exposure}}) = 0.031 \frac{\text{L}}{\text{min}}, \tag{9}$$

  where AF is a parameter defined in the EPA standard which depends on the water gain of the canister and AF_{standard} and CF_{standard} are reference values defined by EPA standards;

- DF is a decay factor taking into account the part of trapped radon in the canister which can decay before being counted. It has been calculated in such a way:

$$DF = \text{e}^{-\ln 2 \cdot \frac{T_{\text{exposure}}}{\tau_{\text{radon}}}} = 0.4 \tag{10}$$

  .

Our estimates of the activities of Radon are reported in Table 16.

	NaI(Tl) Detector	HPGe Detector
Activity [kBq/m^3]	5.17 ± 0.02	2.70 ± 0.04

Table 16: Activity of the Radon in the Air Humidity Sample

Our estimates of the Radon Activity are highly incompatible. This might be due to the approximate nature of our estimation method; hence we conclude that we have a good estimate of the order of magnitude of the radon activity of the air humidity sample and that further and more accurate investigations are required to get a better estimate. It is also important to underline that the estimated Radon activity is at least an order of magnitude greater than the safe threshold, hence spending time in that room could be dangerous!

8 Conclusion

We managed to identify successfully the expected γ transitions in a good variety of both organic and inorganic samples i.e. mushrooms, water, KCl, Autunite and Air Humidity. The estimate of the activity of the sources did not seem to give always reliable results, in some cases, such as that of the air humidity sample, we may think that it was overestimated. This suggests that further investigations and more accurate methods in the activity measurement are required.